

Article

Not peer-reviewed version

Disruption of the *UPC2* Gene Enhances Fluconazole Antifungal Activity by Inhibiting *HAC1* mRNA Splicing in *Candida albicans*

Jinhua Yu , Bingchen Jiang , Juan Xiong , Xiaojing Xu , Liping Xu , [Yuanying Jiang](#) * , [Hui Lu](#) *

Posted Date: 18 March 2026

doi: 10.20944/preprints202603.1460.v1

Keywords: Upc2; unfolded protein response; HAC1 mRNA splicing; *Candida albicans*



Preprints.org is a free multidisciplinary platform providing preprint service that is dedicated to making early versions of research outputs permanently available and citable. Preprints posted at Preprints.org appear in Web of Science, Crossref, Google Scholar, Scilit, Europe PMC.

Copyright: This open access article is published under a [Creative Commons CC BY 4.0 license](#), which permit the free download, distribution, and reuse, provided that the author and preprint are cited in any reuse.

Disclaimer/Publisher's Note: The statements, opinions, and data contained in all publications are solely those of the individual author(s) and contributor(s) and not of MDPI and/or the editor(s). MDPI and/or the editor(s) disclaim responsibility for any injury to people or property resulting from any ideas, methods, instructions, or products referred to in the content.

Article

Disruption of the *UPC2* Gene Enhances Fluconazole Antifungal Activity by Inhibiting *HAC1* mRNA Splicing in *Candida albicans*

Jinhua Yu ¹, Bingchen Jiang ², Juan Xiong ¹, Xiaojing Xu ¹, Liping Xu ¹, Yuanying Jiang ^{1,3,*} and Hui Lu ^{1,3,*}

¹ Department of Pharmacy, Shanghai Tenth People's Hospital, School of Medicine, Tongji University, Shanghai, China

² Shanghai Municipal Hospital of Traditional Chinese Medicine, Shanghai, China

³ Key Laboratory of Pathogen-Host Interaction, Ministry of Education, School of Medicine, Tongji University, Shanghai, China

* Correspondence: jiangyy@tongji.edu.cn (Y.J.); luhui2019@tongji.edu.cn (H.L.)

Abstract

Azole resistance in *Candida albicans* is an increasing clinical challenge. Upc2 is a key transcription factor regulating ergosterol biosynthesis, but its additional roles in azole tolerance remain unclear. This study investigated whether Upc2 contributes to azole resistance through pathways beyond ergosterol synthesis. Chemical sensitivity screening, RNA sequencing, flow cytometry, and molecular assays were performed to compare wild-type *C. albicans* and the *upc2Δ/upc2Δ* mutant under fluconazole (FLC) treatment. The *UPC2* gene deletion increased intracellular calcium levels and downregulated genes in the unfolded protein response (UPR) pathway. Mechanistically, the *UPC2* gene deletion impaired unconventional splicing of *HAC1* mRNA, leading to accumulation of unfolded proteins and enhanced sensitivity to FLC in planktonic growth, hyphal development, and biofilm formation. Our findings reveal that Upc2 regulates proteostasis in *C. albicans*, and its absence enhances FLC efficacy by disrupting the UPR pathway. Targeting Upc2-mediated UPR signaling may represent a promising strategy to combat azole resistance.

Keywords: Upc2; unfolded protein response; *HAC1* mRNA splicing; *Candida albicans*

1. Introduction

Candida albicans is a notable human fungal pathogen capable of colonizing various anatomical sites, including the skin, mucous membranes, and gastrointestinal tract [1,2]. Disruptions in the host's immune system or microbiota can precipitate both localized and systemic infections by *C. albicans*, posing a substantial risk to immunocompromised individuals due to the potential for life-threatening conditions [3]. Azoles represent the primary therapeutic option for candidiasis management. However, due to their fungistatic nature, *C. albicans* demonstrates an intrinsic tolerance to azoles, and extended exposure can facilitate the development of azole resistance [4]. Consequently, there is an imperative need to identify novel molecular targets and develop new antifungal agents to mitigate azole tolerance, counteract drug resistance in *C. albicans*, and thereby augment the efficacy of azole-based treatments [5].

Research has demonstrated that targeting ergosterol synthase enzymes other than Erg11 can further inhibit ergosterol biosynthesis, thereby significantly enhancing the antifungal efficacy of azoles [6]. Pitavastatin, a statin, has been shown to inhibit the activity of 3-hydroxy-3-methylglutaryl-CoA reductase (Hmg1), thereby enhancing the antifungal activity of fluconazole against azole-resistant *Candida* species and even imparting fungicidal properties to fluconazole (FLC) [7]. However, it should be noted that statins may cause adverse nonspecific effects and potential drug interactions

[8]. Terbinafine, an inhibitor of Erg1, exhibits substantial antifungal efficacy against *Aspergillus* and azole-resistant *Candida* species when used in conjunction with azoles [9,10]. Nonetheless, the emergence of resistance to terbinafine among pathogenic fungi limits its clinical application [11]. The small molecule CZ66 has been shown to inhibit Erg251 activity, thereby impeding the synthesis of 14 α -methylsterol and reducing the tolerance of *C. albicans* to azoles, while concurrently augmenting their antifungal efficacy [12]. However, CZ66 is characterized by a short half-life in murine models and does not significantly enhance the in vivo antifungal efficacy of azoles [12]. Consequently, there is an urgent need to develop novel strategies to inhibit ergosterol synthesis and potentiate the antifungal activity of azoles.

Upc2 serves as a pivotal transcription factor in the regulation of ergosterol biosynthesis. Structurally, Upc2 comprises a nuclear localization signal (NLS) at its N-terminus, a DNA-binding domain (DBD), a ligand-binding domain (LBD) at its C-terminus, and an activation loop [13]. Under conditions of normal intracellular ergosterol levels, ergosterol associates with the LBD, while Hsp90 interacts with the activation loop of Upc2, resulting in its retention within the cytoplasm [13,14]. Upon *C. albicans*' exposure to azoles, which cause a reduction in ergosterol levels, ergosterol dissociates from Upc2, inducing conformational changes in the C-terminal activation loop. This conformational change facilitates the dissociation of Hsp90 from Upc2. Subsequently, the nuclear importin Srp1 binds to the NLS of the now free Upc2, mediating its transport into the nucleus. Once inside the nucleus, the DBD of Upc2 binds to sterol response elements (SREs) located in the promoter regions, thereby activating the transcription of ergosterol biosynthesis genes (ERGs) [14].

The transcription factor Upc2 is pivotal in mediating resistance and tolerance to azoles in *Candida* species. Tan et al. demonstrated that Upc2 is capable of sensing intracellular ergosterol levels in fungi, subsequently regulating both the biosynthesis and uptake of ergosterol, which contributes to azole resistance in *Candida* species [14]. Vasicek et al. reported that activation of Upc2 induces azole resistance in *C. albicans*, whereas dysfunction of Upc2 enhances the sensitivity of *C. albicans* to azoles [15]. Wang et al. conducted an analysis of the transcriptional level of the *UPC2* gene in 319 clinical strains of *Candida tropicalis*, revealing a linear positive correlation between the gene's transcriptional level and FLC resistance in *Candida tropicalis* [16]. Li et al. identified that Upc2 is integral to azole resistance in *Candida auris* by facilitating ergosterol biosynthesis and upregulating the expression of the drug transporter Mdr1 [17]. Furthermore, Vu et al. demonstrated that the transcription factor Upc2A in *Candida glabrata* can directly bind to the promoter region of the *CDR1* gene [18]. A previous study demonstrated that the minimum inhibitory concentration (MIC) of FLC was significantly decreased in *C. albicans* mutant with deletions in the *UPC2* gene (*upc2 Δ /upc2 Δ*) [12,19]. These findings suggested that inhibiting the transcriptional activity of Upc2 effectively reduces the tolerance of *C. albicans* to azoles and mitigates azole drug resistance. However, the mechanism by which *C. albicans*, in the absence of the *UPC2* gene, exhibits increased sensitivity to azoles remains unclear.

A recent study has demonstrated that Ellipticine and its analog phiKan 083 specifically target Ncp1, thereby disrupting the interaction between Erg11 and Ncp1. This disruption results in elevated levels of reactive oxygen species (ROS) in *C. albicans*, which subsequently induces protein oxidation and misfolding within the endoplasmic reticulum (ER), culminating in ER stress. The ER stress response facilitates the release of calcium ions (Ca²⁺) from the ER, induces mitochondrial Ca²⁺ accumulation and dysfunction, increases ROS production, and triggers apoptosis in *C. albicans* cells, thereby enhancing the antifungal efficacy of azoles [20]. These findings suggest that the disruption of the ergosterol biosynthetic pathway may contribute to ER stress in *C. albicans*. In this study, we observed that the *C. albicans upc2 Δ /upc2 Δ* mutant demonstrated increased sensitivity to ergosterol synthesis inhibitors and the calcium chelator ethylene glycol tetraacetic acid (EGTA), along with enhanced tolerance to calcium chloride (CaCl₂), in comparison to the wild-type *C. albicans* strain SN152. These findings suggest that the deletion of the *UPC2* gene in *C. albicans* may disrupt Ca²⁺ homeostasis and dysfunction ER. Further investigations revealed that, under FLC treatment, the overall expression of genes involved in the ergosterol synthesis pathway and the unfolded protein response (UPR) pathway was significantly downregulated in the *upc2 Δ /upc2 Δ* mutant compared to

wild-type strain. Our results indicate that the absence of the *UPC2* gene impairs the UPR pathway by reducing the splicing of *HAC1* mRNA, thereby increasing the accumulation of unfolded proteins and ultimately enhancing the antifungal activity of azoles.

2. Materials and Methods

2.1. Strains, Primers, Agents, and Cultural Conditions

All strains, and primers used in this study are detailed in Supplementary Tables S1 and S2. The *C. albicans* strains were cultured in YPD medium, which consists of 2% dextrose (Sangon Biotech, A610219-0500), 1% yeast extract (Oxoid, LP0021B), and 2% peptone (Oxoid, LP0137), at 30 °C for liquid culture growth. For solid medium growth, YPD supplemented with 2% (w/v) agar was used, also at 30 °C unless otherwise specified. For the hyphal growth and biofilm formation assays, RPMI 1640 medium was utilized, comprising 10.4 g/L RPMI-1640 (Sigma-Aldrich, St. Louis, MO, USA), 3.45% MOPS, 0.2% NaHCO₃, and 2% agar, adjusted to a pH of 7.0.

2.2. Antifungal Susceptibility Testing

The MIC assay was conducted following previously established protocols [21]. Briefly, compounds were subjected to a two-fold serial dilution across columns 2 to 11 of a 96-well plate, with 100 µL of liquid being removed from column 11. Subsequently, overnight cultures of *C. albicans* were adjusted to a cell density of 1×10³ cells/mL in YPD medium. A volume of 100 µL of this diluted *C. albicans* cell suspension was then added to each well of the plate. Column 1 served as the positive control, containing 100 µL of YPD and 100 µL of the *C. albicans* cell suspension, while column 12 acted as the blank control with 200 µL of YPD. The plates were incubated at 30 °C for 24 hours without agitation to assess growth inhibition. Prior to the assay, the solutions were homogenized by pipetting, and absorbance was measured at 600 nm (OD₆₀₀) using a spectrophotometer (Thermo Fisher Scientific, Multiskan SkyHigh, USA). The MIC was determined as the lowest concentration of the compound that resulted in a 50% reduction in fungal growth compared to the control wells.

A dose-matrix titration assay was conducted as previously described to assess the synergistic effects of two drugs against *C. albicans* [19,22]. The drugs were serially diluted at a 2-fold ratio in separate 96-well plates, with one drug diluted along the columns and the other along the rows. Equal volumes of the solutions from the two plates were combined, resulting in wells containing various combinations of drug concentrations. Each well was inoculated with 100 µL of an overnight *C. albicans* culture, adjusted to a concentration of 1×10³ cells/mL, with a drug-free growth control included. Following incubation at 30 °C for 24 hours, the optical density at 600 nm (OD₆₀₀) was measured for each well using a spectrophotometer (Thermo Fisher Scientific, Multiskan SkyHigh, USA). The fractional inhibitory concentration index (FICI) was calculated based on the 24-hour MIC results using the following formula: $FICI = MIC_{AB}/MIC_A + MIC_{BA}/MIC_B$. Here, MIC_{AB} represents the MIC of drug A in the presence of drug B; MIC_A refers to the MIC of drug A alone. Similarly, MIC_{BA} represents the MIC of drug B in the presence of drug A; MIC_B refers to the MIC of drug B alone. The interaction between the drugs was classified as synergistic if the FICI was ≤0.5, additive if the FICI ranged from >0.5 to 1.0, indifferent if the FICI ranged from >1.0 to 4.0, and antagonistic if the FICI exceeded 4.0 [23].

2.3. Growth Inhibition Curve Assay

The growth inhibition curve assay was performed following the previously described methodology [24,25]. Briefly, overnight cultures of *C. albicans* colonies were inoculated into YPD medium and adjusted to a cell density of 1×10³ cells/mL. FLC was then serially diluted in a 96-well plate. Each well received 75 µL of the drug solution and 75 µL of the *C. albicans* culture. Wells containing 150 µL of YPD medium served as blank controls. The prepared plate was placed in the Infinite 200 PRO Multifunctional Microplate Reader (Tecan, California, USA) for incubation and analysis. The incubation was conducted at 30 °C, with OD₆₀₀ measured every 15 minutes over a 48-

hour period. Data analysis and graphical representations were generated using GraphPad Prism version 10.1.2.

2.4. Hypha Growth Assay

The hyphal growth assay was conducted as previously described [24,26]. *C. albicans* cells were cultured overnight in YPD medium at 30 °C with agitation until reaching the logarithmic growth phase. The OD₆₀₀ of each culture (SN152 and *upc2Δ/upc2Δ*) was measured and adjusted to ensure equivalent cell densities. The cells were harvested by centrifugation and resuspended in RPMI 1640 medium. Subsequently, the suspension was diluted in RPMI 1640 to achieve a final concentration of 2×10^5 cells/mL. A volume of 100 μL of this cell suspension, along with 100 μL of RPMI 1640 containing serial dilutions of FLC, was added to each well of a 96-well plate. Wells containing only RPMI 1640 served as blank controls. The plates were incubated at 37 °C for 4 hours. Morphological differences between FLC-treated and untreated *C. albicans* cultures were observed and documented at 0, 1, 2, and 4 hours using an inverted microscope (Motic, AE2000, China).

2.5. Biofilm Formation Assay

The biofilm formation assay was conducted as previously described [24,26]. Following overnight culture in YPD medium, *C. albicans* SN152 and *upc2Δ/upc2Δ* cells were resuspended in RPMI 1640 medium and subsequently diluted to a concentration of 10^6 cells/mL. A 96-well plate was utilized, with 100 μL of the cell cultures added to each well. The plates were incubated at 37 °C for 90 minutes to facilitate initial biofilm formation and for 24 hours to allow for mature biofilm development. Post-incubation, the culture medium was carefully removed, and each well was gently washed with sterile phosphate-buffered saline (PBS) to eliminate non-adherent cells. Fresh RPMI 1640 medium, with or without the addition of specific compounds, was then added to the wells, and the cells were cultured at 37 °C for an additional 24 hours. This method necessitated the use of 2,3-bis-(2-methoxy-4-nitro-5-sulfophenyl)-2H-tetrazolium-5-carboxanilide (XTT), which undergoes metabolic reduction to produce a colorimetric, water-soluble formazan product in viable cells [27]. XTT was utilized in conjunction with phenazine methosulfate (PMS). The mixed solution was prepared immediately prior to use, with a ratio of XTT (0.5 mg/mL in DMSO) to PMS (0.32 mg/mL in sterile water) of 9:1, and subsequently stored in a dark environment. Following the completion of drug treatment, the medium was removed from the 96-well plate, and 100 μL of the XTT-PMS mixture was added to each well. The plates were then incubated at 37 °C in the dark for 30 minutes. The XTT-formazan results were analyzed using a microplate reader (Thermo Fisher, Multiskan SkyHigh) at a wavelength of 492 nm. Data were plotted using GraphPad Prism version 10.1.2, displaying the mean relative quantity ± standard deviation.

2.6. RNA Sequencing

The SN152 and *upc2Δ/upc2Δ* mutant cultures were initially grown overnight in YPD medium and subsequently incubated in YPD for an additional 8 hours at 30 °C, with or without the addition of 4 μg/mL FLC. Following incubation, the biological samples were promptly frozen at -80 °C and dispatched for sequencing to BGI Genomics in Shenzhen, China. Differentially expressed genes (DEGs) under both untreated and FLC-treated conditions were identified based on the criteria of $|\log_2$ fold change (FC)| ≥ 1 and Q-value ≤ 0.05 , and these DEGs were depicted using volcano plots.

2.7. Quantitative Real-Time PCR (qRT-PCR) Analysis

C. albicans were cultured overnight and treated with different concentrations of the drugs: 4 μg/mL tunicamycin for 1 hour of culture, 5 mM DTT for 1 hour of culture. The extraction of total RNA were conducted according to the previous study [28]. Quantitative analysis of cDNA was carried out via real-time PCR using TB Green® Premix Ex Taq™ II on a CFX96™ system (Bio-Rad, USA) with the following strategy: 1) 95 °C for 30 s; 2) 95 °C for 5 s, 50 °C for 30 s, and 72 °C for 30 s,

for 40 cycles: 3) 95 °C for 5 s, 50 °C for 30 s, and 72 °C for 30 s. We used *ACT1* as the internal reference gene for normalization. Each sample was subjected to three technical replicates and the expression differences of the target gene were calculated using the $2^{-\Delta\Delta Ct}$ method [29].

2.8. Determination of Unfolded Protein Levels

The quantification of unfolded proteins within cells was conducted using flow cytometry [20,30]. To determine intracellular levels of unfolded proteins, overnight cultures of *C. albicans* were inoculated at a 1:100 dilution and cultivated in the presence or absence of FLC for 4 hours at 30 °C. A 5 μ M concentration of tunicamycin was employed as a positive control for a 4-hour exposure period. Following cultivation, the fungal suspension was resuspended in PBS. Subsequently, 500 μ L of culture (10^7 cells/mL) was treated with either TPE-MI or an equivalent volume of DMSO, and the mixture was incubated in the dark at 37 °C with continuous agitation in a rotating incubator for 30 minutes. Post-incubation, the cells were washed with PBS and filtered through gauze for analysis using a BD FACSVerser flow cytometer (BD Biosciences, New York, USA). The excitation and emission wavelengths for TPE-MI were set at 350 nm and 470 nm, respectively. Forward scatter (FSC) and side scatter (SSC) voltages were adjusted to 220 volts and 250 volts, respectively, to accurately encompass *C. albicans* cells while excluding cellular debris. The gating process was concluded upon reaching the stopping criterion of 10,000 events.

2.9. Detection of *HAC1* mRNA Splicing

The determination of *HAC1* mRNA splicing was conducted as previously described [31]. Subsequently, 128 μ g/mL of FLC was either added to the cultures or omitted, with 5 mM dithiothreitol (DTT) serving as the positive control. After a 2-hour incubation period following compound addition, cells were collected via centrifugation. Total RNA was extracted using the Yeast RNA Extraction Kit (Zymo Research, R1002). The quality and integrity of the RNA were assessed using the Agilent 2100 Bioanalyzer and formaldehyde gel electrophoresis. For the gel preparation, 0.28 g of agarose was dissolved in 20 mL of 1 \times MOPS buffer (comprising 2.5 mL of 10 \times MOPS buffer and 22.5 mL of DEPC-treated water). Upon complete dissolution, 292 μ L of formaldehyde and 2 μ L of TS-GelRed were gently mixed into the solution, which was then poured onto the gel plate. Electrophoresis was conducted in 1 \times MOPS buffer at 80 V for 40 minutes, and RNA visualization was achieved using UV light. The integrity of the RNA was confirmed by the clear observation of the 28S and 18S bands, with the 28S band exhibiting twice the brightness of the 18S band. Subsequently, a *HAC1*-specific reverse primer was utilized to synthesize complementary DNA (cDNA), followed by polymerase chain reaction (PCR) amplification of the cDNA samples. Post-PCR, the relative abundance of *HAC1* transcripts was assessed through DNA electrophoresis on a 3% agarose gel.

3. Results

3.1. Deletion of the *UPC2* Gene in *C. albicans* Disrupts the Ca^{2+} Homeostasis

We utilized a MIC assay to assess the susceptibility of the *C. albicans* wild-type strain SN152 and the *upc2* Δ /*upc2* Δ mutant to a panel of 20 compounds (Figure 1a). These compounds target various cellular processes, including the cell wall, cell membrane, osmotic pressure, endoplasmic reticulum stress, DNA damage, oxidative stress, iron homeostasis, and calcium homeostasis. The *upc2* Δ /*upc2* Δ mutant exhibited significantly heightened sensitivity to three inhibitors of ergosterol biosynthesis: FLC (an Erg11 inhibitor) [32], terbinafine (an Erg1 inhibitor) [33,34], and fluvastatin (an Hmg1 inhibitor) [33]. These results corroborate previous findings, indicating that the deletion of *Upc2* markedly enhances the sensitivity of *C. albicans* to inhibitors of ergosterol synthesis.

The *upc2* Δ /*upc2* Δ mutant exhibits increased sensitivity to three drugs associated with Ca^{2+} homeostasis, including geldanamycin, an Hsp90 inhibitor [35,36], and the calcineurin inhibitors cyclosporine A and tacrolimus [37,38] (Figure 1a). We further performed a dose-matrix titration assay on SN152 and the *upc2* Δ /*upc2* Δ mutant to calculate the FICI between geldanamycin and FLC. The

results indicated that geldanamycin and FLC demonstrated an indifferent interaction against SN152 (FICI=2), whereas they exhibited a synergistic interaction against the *upc2Δ/upc2Δ* mutant (FICI=0.25)(Figure 1b,c). These findings suggest that the deletion of the *UPC2* gene in *C. albicans* may disrupt Ca^{2+} homeostasis of the fungus.

To further substantiate this inference, we examined the sensitivity of the *upc2Δ/upc2Δ* mutant to the Ca^{2+} chelator EGTA and $CaCl_2$. Our findings indicate that the *upc2Δ/upc2Δ* mutant demonstrated decreased sensitivity to EGTA and heightened sensitivity to $CaCl_2$ (Figure 1a). Additionally, we administered varying concentrations of Ca^{2+} and subsequently determined the MIC of SN152 and *upc2Δ/upc2Δ* in the presence of FLC and geldanamycin (Figure 1d,e). Upon Ca^{2+} supplementation, the sensitivity of SN152 to FLC increased, whereas the sensitivity of *upc2Δ/upc2Δ* to FLC remained unchanged (Figure 1d). Notably, after the addition of 1 mM $CaCl_2$, the MIC of *upc2Δ/upc2Δ* for geldanamycin increased from 16 μ M to 32 μ M, and with the addition of 25 mM and 50 mM $CaCl_2$, the MIC exceeded 256 μ M (Figure 1f). These findings suggest that the deletion of the *UPC2* gene in *C. albicans* results in an elevated intracellular Ca^{2+} concentration within *C. albicans* cells

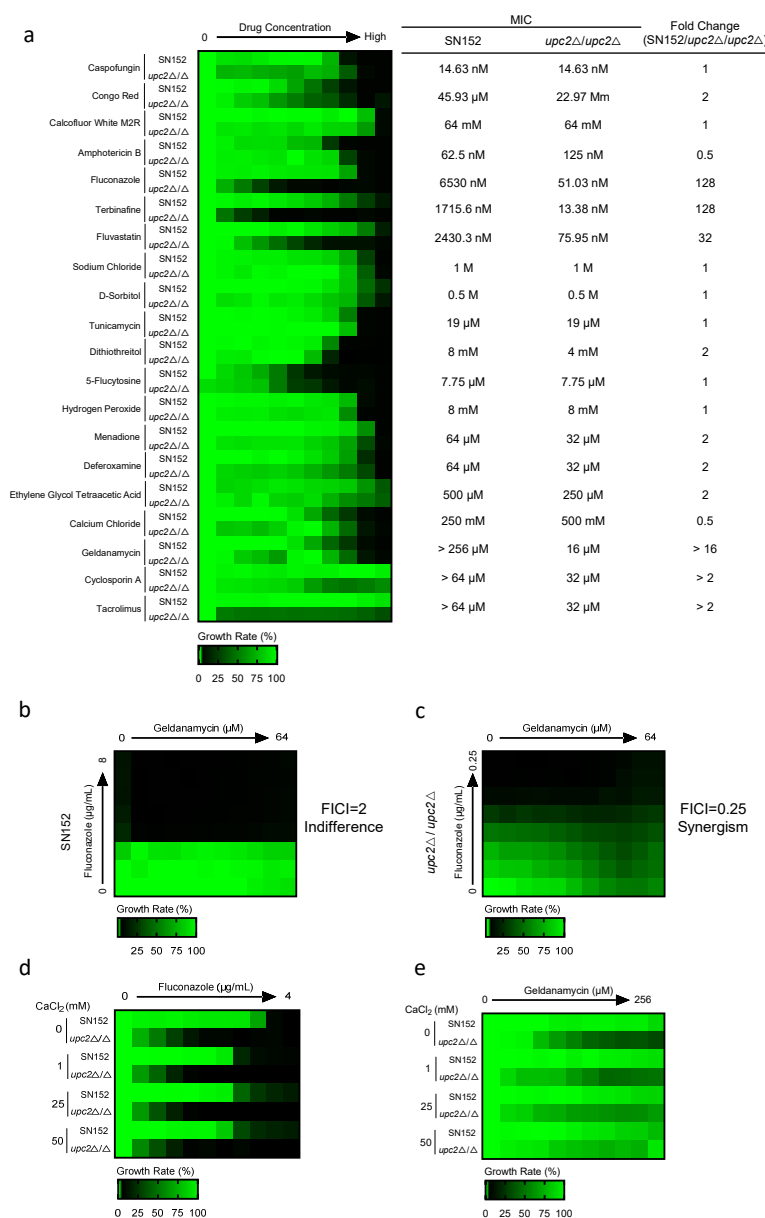


Figure 1. Deletion of the *UPC2* gene in *C. albicans* disrupts the Ca^{2+} homeostasis. (a) MIC assay to assess the susceptibility of the *C. albicans* wild-type strain SN152 and the *upc2* Δ /*upc2* Δ mutant to a panel of 20 compounds. (b) (c) Dose matrix titration experiments of SN152 and *upc2* Δ /*upc2* Δ under different compound treatments. All strains were cultured in YPD medium at 30 °C for 24 hours. (d) (e) After supplementing with 1 mM, 25 mM, and 50 mM CaCl_2 , the MIC values of fluconazole and geldanamycin for SN152 and *upc2* Δ /*upc2* Δ were determined. All strains were cultured in YPD medium at 30 °C for 24 hours.

3.2. The Deletion of *UPC2* Gene in *C. albicans* Affects the Expression of the ER Stress Related Genes

The synthesis of ergosterol in *C. albicans* occurs within the ER, and increased intracellular Ca^{2+} concentrations may exacerbate ER stress in this organism [20]. Consequently, we propose the hypothesis that the deletion of the *UPC2* gene in *C. albicans* could induce ER stress. To evaluate this hypothesis, we utilized RNA sequencing (RNA-seq) technology to perform a transcriptomic analysis of *C. albicans* subjected to FLC treatment. Our findings indicate that, in comparison to the SN152 strain, the gene expression profile of the *upc2* Δ /*upc2* Δ mutant exhibited significant alterations. Under FLC treatment, 1,817 DEGs were identified, comprising 867 upregulated and 950 downregulated genes (Figure 2a). Gene Ontology (GO) analysis of molecular function and biological processes revealed an enrichment of DEGs in unfolded protein binding (Figure 2b). Gene Set Enrichment Analysis (GSEA) demonstrated that the Normalized Enrichment Scores (NES) for unfolded protein binding pathway was -1.61 (Figure 2c). To mitigate or manage ER stress, *C. albicans* cells utilize the UPR pathway, which plays a crucial role in restoring homeostasis and normal ER function [39]. The molecular function of unfolded protein binding is executed by ER chaperones, such as BiP, which detect and bind to misfolded proteins, thereby initiating the UPR and facilitating protein refolding during ER stress [40]. In our study, we further examined the genes associated with unfolded protein binding in the FLC treatment. We identified a total of 76 genes regulated by the unfolded protein binding [41] and calculated the fold change in expression for each gene in the SN152 and *upc2* Δ /*upc2* Δ strains, based on transcripts per million (TPM) (Figure 2d). these findings suggested that the deletion of *UPC2* gene in *C. albicans* affects the expression of the ER stress related genes.

3.3. The Deletion of *UPC2* Gene Inhibits the UPR Pathway in *C. albicans*

We selected five representative genes associated with the UPR pathway, specifically those involved in translocation and protein folding, and validated their expression through quantitative PCR analysis. Under FLC treatment, the *SEC12* and *HAC1* genes were notably overexpressed in the *upc2* Δ /*upc2* Δ strain (Figure 3a). To assess whether the absence of the *UPC2* gene influences the levels of unfolded proteins, we employed flow cytometry. Tetrathiophene maleimide (TPE-MI), a fluorescent dye with aggregation-induced emission properties capable of penetrating the cell membrane, was utilized to measure unfolded protein content [30,42]. As proteins unfold, cysteine residues previously buried in the folded core become exposed. This dye binds to the sulfhydryl groups of misfolded proteins, thereby emitting fluorescence [43]. Tunicamycin, an ER stress inducer known to inhibit N-glycosylation and promote the accumulation of misfolded proteins, was used as a positive control [44]. Our analysis revealed that the fluorescence levels in both the control group (DMSO) and the FLC-treated group were markedly elevated in the *upc2* Δ /*upc2* Δ strain compared to the SN152 strain (Figure 3b,c). This observation suggests that the deletion of the *UPC2* gene results in an accumulation of unfolded proteins, and that exposure to FLC exacerbates this accumulation.

To mitigate ER stress and restore protein folding capacity, cells initiate the UPR as an adaptive mechanism [45]. The ER transmembrane receptor Ire1, possessing dual protein kinase and ribonuclease activities, is adept at detecting the excessive accumulation of unfolded proteins within the ER. It becomes activated through dimerization, oligomerization, and autophosphorylation across the ER membrane [46,47]. In response to ER stress, the activated Ire1 cleaves *HAC1* mRNA in yeast in a spliceosome-independent manner, thereby excising the intron sequences [48]. In the context of ER stress in *C. albicans*, Ire1 excises the intron fragment, and the resulting exons are ligated by tRNA ligase to produce *HAC1^s* mRNA (Figure 3d). The precursor *HAC1* mRNA and its spliced variant are

designated as $HAC1^u$ (unspliced) and $HAC1^s$ (spliced), respectively, distinguished by a 19-nucleotide fragment [31].

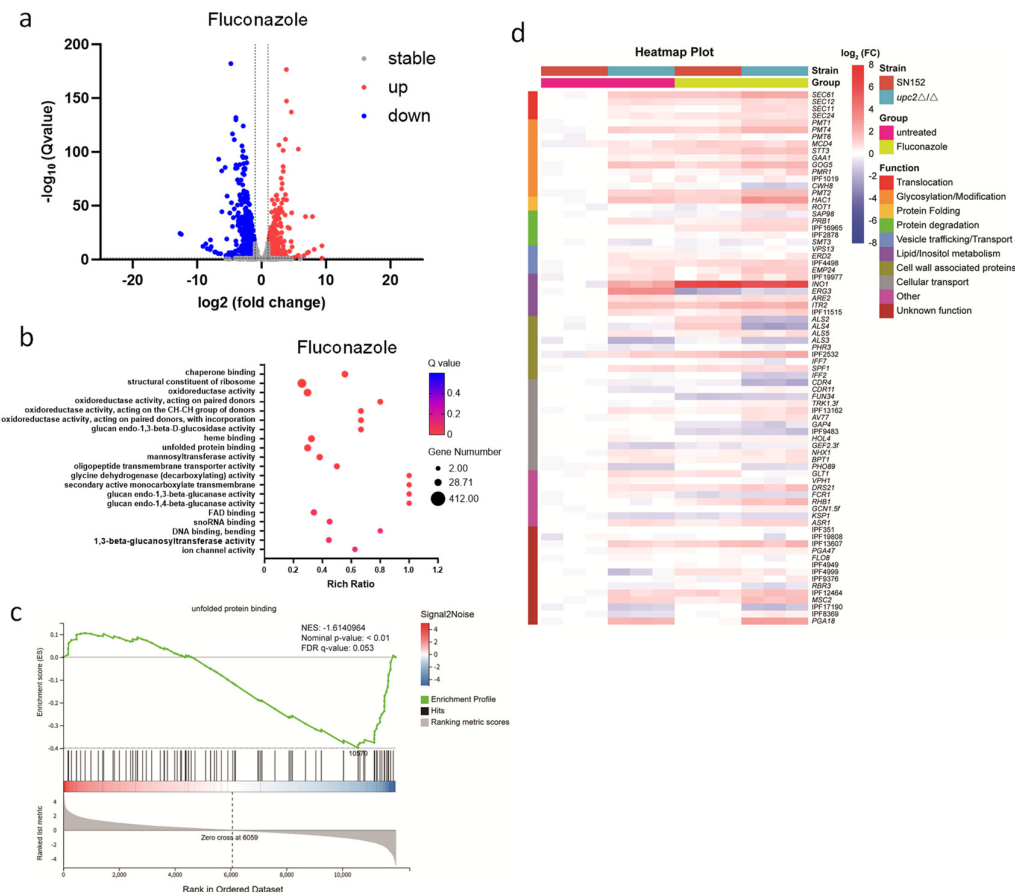


Figure 2. The deletion of *UPC2* gene in *C. albicans* affects the expression of the ER stress related genes. (a) When treated with 4 $\mu\text{g}/\text{mL}$ fluconazole for 8 hours, SN152 and *upc2* Δ /*upc2* Δ both showed differential genes. The differentially expressed genes were analyzed through RNA-seq. Each group of samples had 3 biological replicates, and the screening criteria for differential genes were $|\log_2\text{FC}| \geq 1$ and $Q \leq 0.05$. (b) Under the action of fluconazole, the DEGs of SN152 and *upc2* Δ /*upc2* Δ were enriched in the unfolded protein binding pathway. GO molecular function enrichment analysis of DEGs. (c) In GSEA of the DEGs, the gene set related to unfolded protein binding was downregulated. (d) TPM analysis of the DEGs.

In this study, we assessed the splicing ratio of *HAC1* mRNA in SN152 and *upc2* Δ /*upc2* Δ strains under both untreated and FLC-treated conditions. Dithiothreitol (DTT) was utilized as a positive control. PCR products were resolved on a 3% agarose gel and visualized under UV light. The relative levels of the spliced *HAC1*^s transcript were quantified by calculating the ratio of *HAC1*^s to the sum of *HAC1*^u and *HAC1*^s. Our results indicated that, following 60 and 120 minutes of FLC treatment, the relative levels of *HAC1*^s transcript in the *upc2* Δ /*upc2* Δ strain were significantly reduced compared to those in the SN152 strain (Figure 3e,f). These findings suggest that the *UPC2* gene deletion impairs *HAC1* mRNA splicing in *C. albicans*. This impairment likely results in the accumulation of unfolded proteins, thereby increasing the *upc2* Δ /*upc2* Δ strain's sensitivity to FLC.

3.4. The Deletion of *UPC2* Gene Hyphal Growth of *C. albicans* and Enhance FLC Against *C. albicans* Biofilm

C. albicans exhibits a hyphal morphology that serves as a crucial virulence factor, facilitating invasion by breaching the mucosal barrier and penetrating the surfaces of biomedical materials such

as medical silicone, thereby enabling the invasion of deep host tissues [49–51]. To investigate whether the deletion of *UPC2* gene influences hyphal growth, *C. albicans* SN152 and *upc2Δ/upc2Δ* strains was cultured in RPMI 1640 medium at 37 °C, and hyphal development was observed at 0, 2, and 4 hours. In the absence of drug treatment, both SN152 and *upc2Δ/upc2Δ* strains were capable of hyphal growth, with no significant differences in hyphal morphology observed at the same time points (Figure 4a). Notably, we observed a tendency for the hyphae of the *upc2Δ/upc2Δ* strain to aggregate. After 4 hours, the proportion of cell groups containing ten aggregated cells was higher in the *upc2Δ/upc2Δ* strain compared to the SN152 strain (Figure 4b). Upon treatment with FLC, the hyphal growth of the *upc2Δ/upc2Δ* strain was more significantly inhibited than that of SN152, with the disparity increasing over time (Figure 4c,d). These findings suggest that the absence of the *UPC2* gene impairs hyphal growth under FLC-induced stress.

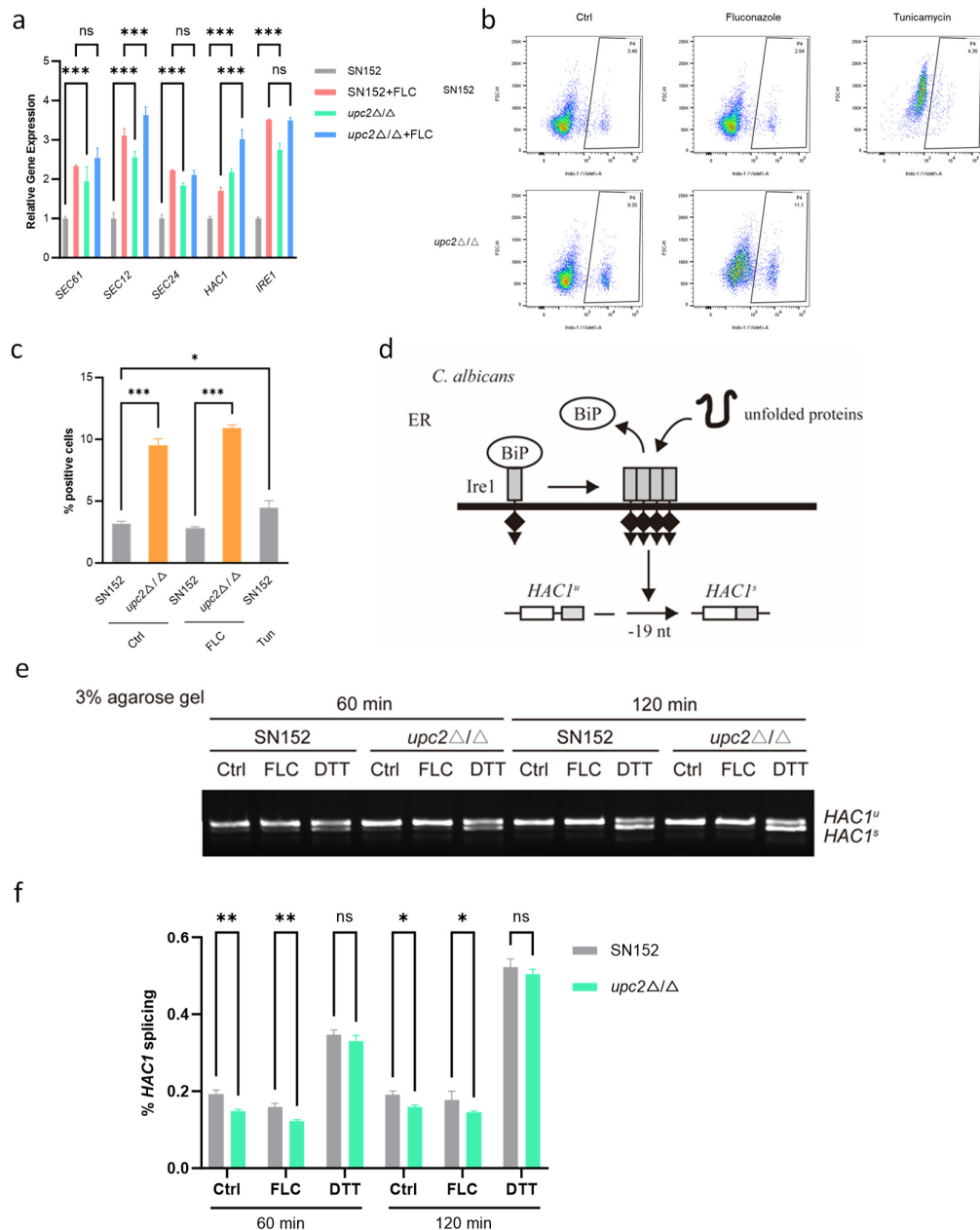


Figure 3. The deletion of *UPC2* gene inhibits the UPR pathway in *C. albicans*. (a) The absence of the *UPC2* leads to the upregulation of some genes in the unfolded protein binding pathway. The expression of genes in

the unfolded protein binding pathway was analyzed using qRT-PCR. 128 ng/mL fluconazole was applied to SN152 and *upc2Δ/upc2Δ* for 8 hours. Data are expressed as mean ± SD for biological triplicates. Significance was determined by two-way ANOVA; ****p* < 0.001. (b) The content of *upc2Δ/upc2Δ* unfolded proteins was higher than that of SN152 unfolded proteins. The content of unfolded proteins was determined using flow cytometry. 128 ng/mL fluconazole and 5 μM tunicamycin were treated for 4 hours, with FSC at 220V, SSC at 250V, and Indo-1 at 360V. (c) Statistical analysis of the content of unfolded proteins. The data are presented as the mean ± SD for biological triplicates. Significance was determined by one-way ANOVA; **p* < 0.033, ***p* < 0.002, ****p* < 0.001. (d) Schematic diagram of translational control of *HAC1* mRNA in *C. albicans*. (e) The splicing rate of *HAC1* mRNA in SN152 and *upc2Δ/upc2Δ* was analyzed using RT-PCR. 128 ng/mL fluconazole and 5 mM DTT were used as positive controls. (f) Statistical analysis of the splicing rate of *HAC1* mRNA at 60 minutes and 120 minutes. The data were expressed as the average value ± standard deviation of 3 biological replicates. Significance was determined by two-way ANOVA; **p* < 0.033, ***p* < 0.002.

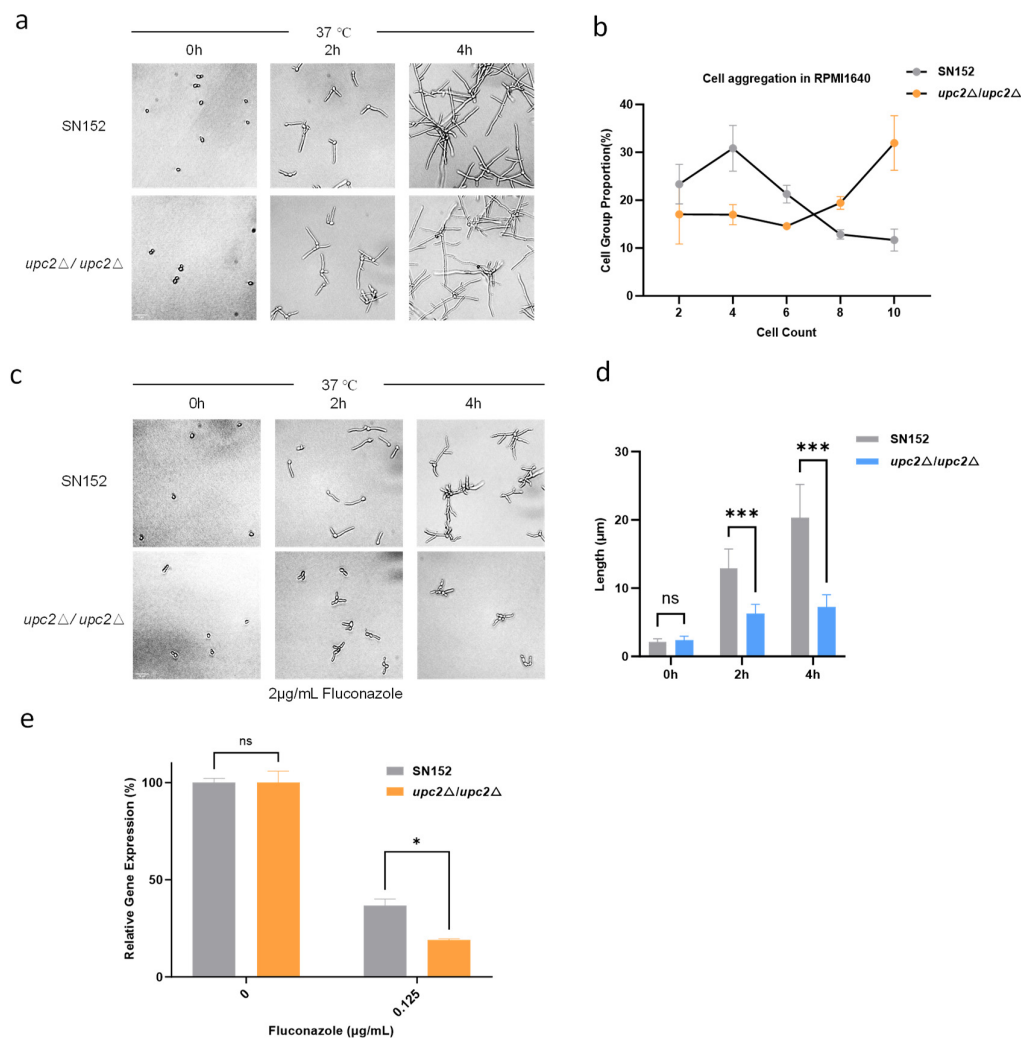


Figure 4. The deletion of *UPC2* gene hyphal growth of *C. albicans* and enhance FLC against *C. albicans* biofilm. (a) The growth conditions of the hyphae at different times, with a scale of 20 μm. (b) The proportion of cell clusters after 4 hours of cell aggregation, for each fungus, 60 or more cells were counted. The data are presented as the average value ± standard deviation of biological replicates. (c) Growth of SN152 and *upc2Δ/upc2Δ* hyphae at 0 hours, 2 hours, and 4 hours, with a scale of 20 μm. SN152 and *upc2Δ/upc2Δ* were cultured in RPMI 1640 medium at 37 °C and 2 μg/mL fluconazole. (d) Length of SN152 and *upc2Δ/upc2Δ* hyphae at 0 hours, 2 hours, and 4 hours, with data presented as the average value ± standard deviation of 30 biological replicates. Significance was determined by two-way ANOVA; ****p* < 0.001. (e) The absence of *UPC2* significantly

reduced the sensitivity of the biofilm formed during the growth of *C. albicans* to fluconazole. SN152 and *upc2Δ/upc2Δ* were cultured at 37 °C in RPMI 1640 medium. The data were expressed as the average value ± standard deviation of 2 biological replicates. Significance was determined by two-way ANOVA; **p* < 0.033, ***p* < 0.002, ****p* < 0.001.

Biofilms composed of yeast cells, pseudohyphae, and hyphae are initiated through the adsorption and adhesion of *C. albicans* yeast cells to a substrate. Once established, these biofilms exhibit a high tolerance to antifungal drugs, posing a substantial challenge in clinical treatment [52–55]. To elucidate the role of Upc2 in biofilm formation under FLC pressure, we employed the XTT reduction assay to assess the inhibitory effects of FLC on the biofilm formation of SN152 and *upc2Δ/upc2Δ* strains. XTT, a tetrazole salt, undergoes bioreduction to produce a water-soluble formazan, and is routinely utilized for the quantitative evaluation of *C. albicans* biofilms by measuring cellular activity [56,57]. Our findings indicate that at a concentration of 0.125 μg/mL FLC, the biofilm formation of the *upc2Δ/upc2Δ* mutant was significantly inhibited compared to that of SN152 (Figure 4e).

4. Discussion

In this study, we examined the mechanism by which the deletion of the *UPC2* gene enhances the antifungal efficacy of FLC against *C. albicans*. Our findings indicate that the deletion of the *UPC2* gene disrupts Ca²⁺ homeostasis, impairs the UPR pathway by reducing *HAC1* mRNA splicing, and ultimately results in the accumulation of unfolded proteins. This accumulation synergizes with FLC to exert fungicidal effects on *C. albicans*. These results offer novel insights into the mechanisms underlying azole tolerance and identify potential therapeutic targets for addressing drug resistance in fungal infections.

Our preliminary chemical screening indicated that, beyond the inhibitors of ergosterol synthesis, the *upc2Δ/upc2Δ* mutant demonstrated markedly heightened sensitivity to compounds affecting Ca²⁺ homeostasis, notably the Hsp90 inhibitor geldanamycin. Through combination drug assays and Ca²⁺ supplementation experiments, we verified that the deletion of the *UPC2* gene results in increased intracellular Ca²⁺ concentrations in *C. albicans*. This observation aligns with previous studies that have shown Hsp90 to physically interact with Upc2 and regulate its transcriptional activity [13,14]. Hsp90 is recognized for its crucial role in maintaining proteostasis and modulating the activity of numerous signaling proteins involved in drug resistance [58–61]. In *C. albicans*, Hsp90 regulates echinocandin resistance via calcineurin, and depletion of Hsp90 mimics the azole sensitivity seen in calcineurin and protein kinase C mutants [36,62]. Our findings expand upon these observations by demonstrating that Upc2 is functionally associated with Ca²⁺ homeostasis downstream of Hsp90, and that disruption of this interaction contributes to increased sensitivity to azoles.

The ER serves as the primary organelle responsible for protein folding, lipid synthesis, and Ca²⁺ storage within eukaryotic cells [63]. Disruptions in ER homeostasis, such as the accumulation of misfolded proteins or disturbances in Ca²⁺ signaling, activate the UPR pathway, an adaptive signaling pathway aimed at restoring proteostasis [39]. Our transcriptomic analysis demonstrated that, under FLC treatment, genes associated with the UPR pathway were significantly downregulated in the *upc2Δ/upc2Δ* mutant relative to the wild-type strain. Notably, we observed that the absence of the *UPC2* gene compromises the splicing of *HAC1* mRNA, a crucial step for the UPR pathway activation. In yeast, the ER transmembrane kinase/ribonuclease Ire1 initiates UPR signaling through the unconventional splicing of *HAC1* mRNA, resulting in the production of the active transcription factor Hac1, which subsequently induces the expression of UPR target genes [46,48]. The diminished splicing efficiency of *HAC1* mRNA in the *upc2Δ/upc2Δ* mutant leads to impaired the UPR pathway activation, resulting in the accumulation of unfolded proteins. This accumulation of unfolded proteins creates a proteotoxic stress that synergizes with FLC to inhibit fungal growth.

Calcium signaling has emerged as a promising target for combination antifungal therapy [64]. Several studies have shown that targeting Ca²⁺ signaling pathways, such as using Ca²⁺ channel

blockers or calcineurin inhibitors, can significantly enhance the efficacy of azoles against *C. albicans*, particularly in biofilm-associated infections [5,61]. Our finding that the *UPC2* gene deletion disrupts Ca^{2+} homeostasis is consistent with this body of work and provides another link between ergosterol biosynthesis, Ca^{2+} signaling, and azole tolerance. The observation that supplementation with exogenous Ca^{2+} increased the MIC of geldanamycin in the *upc2Δ/upc2Δ* mutant further supports the conclusion that the increased sensitivity is due to elevated basal intracellular Ca^{2+} levels. This suggests that combining Upc2 inhibitors with Ca^{2+} signaling blockers could be an effective strategy for enhancing azole efficacy.

An important implication of our study is that targeting the UPR pathway offers a promising therapeutic strategy to overcome azole tolerance. Traditionally, efforts to address azole resistance have predominantly concentrated on inhibiting ergosterol biosynthesis [12,65]. However, our findings indicate that interfering with the UPR pathway, specifically through the splicing of *HAC1* mRNA, can significantly enhance the antifungal efficacy of FLC. This aligns with recent research demonstrating that disrupting the interaction between Erg11 and Ncp1 augments azole effectiveness by inducing ER stress and elevating ROS production [20]. Collectively, these studies propose that impairing the capacity of *C. albicans* to manage proteotoxic stress represents a promising strategy for converting fungistatic azoles into fungicidal agents.

Several questions remain to be addressed in future studies. First, the precise molecular mechanism by which Upc2 regulates *HAC1* mRNA splicing remains unclear. It is possible that Upc2 directly or indirectly regulates the expression of components of the UPR pathway, or that the effect is secondary to changes in ergosterol content and membrane fluidity. Second, it would be important to determine whether inhibiting Upc2 or the UPR pathway is effective against azole-resistant clinical isolates of *C. albicans* and other pathogenic *Candida* species such as *C. auris*, where Upc2 overexpression is frequently associated with drug resistance [17]. Third, in vivo studies are needed to evaluate the efficacy of combining Upc2 inhibitors with FLC in animal models of candidiasis. Finally, it would be interesting to explore whether there are synergistic interactions between UPR inhibitors and other classes of antifungal agents beyond azoles.

5. Conclusions

In conclusion, our study demonstrates that the absence of the *UPC2* gene in *C. albicans* enhances the antifungal effect of FLC by reducing *HAC1* mRNA splicing, impairing the UPR pathway, and increasing the accumulation of unfolded proteins. These findings reveal a previously unrecognized role for Upc2 in regulating proteostasis and Ca^{2+} homeostasis beyond its canonical function in controlling ergosterol biosynthesis. Our results suggest that developing inhibitors targeting the UPR pathway could be an effective strategy to enhance the efficacy of FLC and overcome azole resistance in *C. albicans*.

Supplementary Materials: The following supporting information can be downloaded at: Preprints.org, Table S1: Strains were used in this study; Table S2: Primers were used in this study.

Author Contributions: Conceptualization, Y.J. and H.L.; methodology, J.Y.; validation, B.J., J.X., L.X., and X.X.; formal analysis, J.Y.; investigation, J.Y.; writing—original draft preparation, J.Y.; writing—review and editing, J.Y., B.J., J.X., L.X., X.X., Y.J., and H.L.; supervision, Y.J. and H.L.; project administration, Y.J. and H.L.; funding acquisition, H.L.. All authors have read and agreed to the published version of the manuscript.

Funding: This study received financial support from the National Natural Science Foundation of China (No. 82574464).

Institutional Review Board Statement: Not applicable.

Informed Consent Statement: Not applicable.

Data Availability Statement: The RNA-Seq data from this study has been submitted to the NCBI under the BioProject ID: PRJNA1288166 (<http://www.ncbi.nlm.nih.gov/bioproject/1288166>).

Conflicts of Interest: The authors declare no conflicts of interest.

Abbreviations

The following abbreviations are used in this manuscript:

Hmg1	3-hydroxy-3-methylglutaryl-CoA reductase
FLC	fluconazole
NLS	nuclear localization signal
DBD	DNA-binding domain
LBD	ligand-binding domain
SREs	sterol response elements
ERGs	ergosterol biosynthesis genes
MIC	minimum inhibitory concentration
ROS	reactive oxygen species
ER	endoplasmic reticulum
Ca ²⁺	calcium ions
EGTA	ethylene glycol tetraacetic acid
UPR	unfolded protein response

References

1. Chen, H., et al., The regulation of hyphae growth in *Candida albicans*. *Virulence*, 2020. 11(1): p. 337-348.
2. Lu, H., et al., Candidiasis: From cutaneous to systemic, new perspectives of potential targets and therapeutic strategies. *Adv Drug Deliv Rev*, 2023. 199: p. 114960.
3. Ho, J., et al., *Candida albicans* and candidalysin in inflammatory disorders and cancer. *Immunology*, 2021. 162(1): p. 11-16.
4. Feng, Y., et al., Understanding fluconazole tolerance in *Candida albicans*: implications for effective treatment of candidiasis and combating invasive fungal infections. *J Glob Antimicrob Resist*, 2023. 35: p. 314-321.
5. Lu, H., et al., *Candida albicans* targets that potentially synergize with fluconazole. *Crit Rev Microbiol*, 2021. 47(3): p. 323-337.
6. Xiong, J., H. Lu, and Y. Jiang, Mechanisms of Azole Potentiation: Insights from Drug Repurposing Approaches. *ACS Infect Dis*, 2025.
7. Li, W., et al., Pitavastatin Calcium Confers Fungicidal Properties to Fluconazole by Inhibiting Ubiquinone Biosynthesis and Generating Reactive Oxygen Species. *Antioxidants (Basel)*, 2024. 13(6).
8. Thompson, P.D., et al., Statin-Associated Side Effects. *J Am Coll Cardiol*, 2016. 67(20): p. 2395-2410.
9. Khodavandi, A., et al., Possible mechanisms of the antifungal activity of fluconazole in combination with terbinafine against *Candida albicans*. *Pharm Biol*, 2014. 52(12): p. 1505-9.
10. Bidaud, A.L., et al., In Vitro Antifungal Combination of Terbinafine with Itraconazole against Isolates of Trichophyton Species. *Antimicrob Agents Chemother*, 2022. 66(1): p. e0144921.
11. Canete-Gibas, C.F., et al., Terbinafine-Resistant Dermatophytes and the Presence of Trichophyton indotineae in North America. *J Clin Microbiol*, 2023. 61(8): p. e0056223.
12. Lu, H., et al., A Small Molecule Inhibitor of Erg251 Makes Fluconazole Fungicidal by Inhibiting the Synthesis of the 14 α -Methylsterols. *mBio*, 2023. 14(1): p. e0263922.
13. Yang, H., et al., Structural mechanism of ergosterol regulation by fungal sterol transcription factor Upc2. *Nat Commun*, 2015. 6: p. 6129.
14. Tan, L., et al., Structural basis for activation of fungal sterol receptor Upc2 and azole resistance. *Nat Chem Biol*, 2022. 18(11): p. 1253-1262.
15. Vasicek, E.M., et al., UPC2 is universally essential for azole antifungal resistance in *Candida albicans*. *Eukaryot Cell*, 2014. 13(7): p. 933-46.
16. Wang, D., et al., *Candida tropicalis* distribution and drug resistance is correlated with ERG11 and UPC2 expression. *Antimicrob Resist Infect Control*, 2021. 10(1): p. 54.

17. Li, J., et al., Upc2-mediated mechanisms of azole resistance in *Candida auris*. *Microbiol Spectr*, 2024. 12(2): p. e0352623.
18. Vu, B.G., G.H. Thomas, and W.S. Moye-Rowley, Evidence that Ergosterol Biosynthesis Modulates Activity of the Pdr1 Transcription Factor in *Candida glabrata*. *mBio*, 2019. 10(3).
19. Zhen, C., et al., Otilonium Bromide Exhibits Potent Antifungal Effects by Blocking Ergosterol Plasma Membrane Localization and Triggering Cytotoxic Autophagy in *Candida Albicans*. *Adv Sci (Weinh)*, 2024. 11(35): p. e2406473.
20. Li, W., et al., Impairing the interaction between Erg11 and cytochrome P450 reductase Ncp1 enhances azoles' antifungal activities. *Nat Commun*, 2025. 16(1): p. 6821.
21. Hang, S., et al., Galactose Inhibits the Translation of Erg1 that Enhances the Antifungal Activities of Azoles Against *Candida albicans*. *Antibiotics (Basel)*, 2025. 14(8).
22. Xiong, J., et al., Halofantrine Hydrochloride Acts as an Antioxidant Ability Inhibitor That Enhances Oxidative Stress Damage to *Candida albicans*. *Antioxidants (Basel)*, 2024. 13(2).
23. Orhan, G., et al., Synergy tests by E test and checkerboard methods of antimicrobial combinations against *Brucella melitensis*. *J Clin Microbiol*, 2005. 43(1): p. 140-3.
24. Fang, T., et al., Unexpected Inhibitory Effect of Octenidine Dihydrochloride on *Candida albicans* Filamentation by Impairing Ergosterol Biosynthesis and Disrupting Cell Membrane Integrity. *Antibiotics (Basel)*, 2023. 12(12).
25. Chai, X., et al., Integrating ensemble machine learning and multi-omics approaches to identify Dp44mT as a novel anti-*Candida albicans* agent targeting cellular iron homeostasis. *Front Pharmacol*, 2025. 16: p. 1574990.
26. Wu, H., et al., Isobavachalcone Exhibits Potent Antifungal Efficacy by Inhibiting Enolase Activity and Glycolysis in *Candida albicans*. *ACS Infect Dis*, 2024. 10(8): p. 3059-3070.
27. Gulati, M., et al., In Vitro Culturing and Screening of *Candida albicans* Biofilms. *Curr Protoc Microbiol*, 2018. 50(1): p. e60.
28. Wang, H., et al., Myriocin enhances the antifungal activity of fluconazole by blocking the membrane localization of the efflux pump Cdr1. *Front Pharmacol*, 2022. 13: p. 1101553.
29. Livak, K.J. and T.D. Schmittgen, Analysis of relative gene expression data using real-time quantitative PCR and the 2(-Delta Delta C(T)) Method. *Methods*, 2001. 25(4): p. 402-8.
30. Zhang, S. and Y. Hong, Measuring Cysteine Exposure in Unfolded Proteins with Tetraphenylethene Maleimide and its Analogs. *Methods Mol Biol*, 2022. 2378: p. 3-18.
31. Uppala, J.K. and M. Dey, Detection of HAC1 mRNA Splicing by RT-PCR in *Saccharomyces cerevisiae*. *Methods Mol Biol*, 2022. 2378: p. 101-110.
32. Ostrosky-Zeichner, L., et al., An insight into the antifungal pipeline: selected new molecules and beyond. *Nat Rev Drug Discov*, 2010. 9(9): p. 719-27.
33. Gianni, C., Update on antifungal therapy with terbinafine. *G Ital Dermatol Venereol*, 2010. 145(3): p. 415-24.
34. Ryder, N.S., Terbinafine: mode of action and properties of the squalene epoxidase inhibition. *Br J Dermatol*, 1992. 126 Suppl 39: p. 2-7.
35. Roe, S.M., et al., Structural basis for inhibition of the Hsp90 molecular chaperone by the antitumor antibiotics radicicol and geldanamycin. *J Med Chem*, 1999. 42(2): p. 260-6.
36. Singh, S.D., et al., Hsp90 governs echinocandin resistance in the pathogenic yeast *Candida albicans* via calcineurin. *PLoS Pathog*, 2009. 5(7): p. e1000532.
37. Handschumacher, R.E., et al., Cyclophilin: a specific cytosolic binding protein for cyclosporin A. *Science*, 1984. 226(4674): p. 544-7.
38. Baldari, C.T., et al., Cyclosporin A blocks calcium-dependent pathways of gene activation. *J Biol Chem*, 1991. 266(28): p. 19103-8.
39. Senft, D. and Z.A. Ronai, UPR, autophagy, and mitochondria crosstalk underlies the ER stress response. *Trends Biochem Sci*, 2015. 40(3): p. 141-8.
40. Kopp, M.C., et al., UPR proteins IRE1 and PERK switch BiP from chaperone to ER stress sensor. *Nat Struct Mol Biol*, 2019. 26(11): p. 1053-1062.

41. Wimalasena, T.T., et al., Impact of the unfolded protein response upon genome-wide expression patterns, and the role of Hac1 in the polarized growth, of *Candida albicans*. *Fungal Genet Biol*, 2008. 45(9): p. 1235-47.
42. Chen, M.Z., et al., A thiol probe for measuring unfolded protein load and proteostasis in cells. *Nat Commun*, 2017. 8(1): p. 474.
43. Shi, Y., et al., Helical Sulfonyl- γ -AApeptides with Aggregation-Induced Emission and Circularly Polarized Luminescence. *J Am Chem Soc*, 2019. 141(32): p. 12697-12706.
44. Xiao, H., J.M. Smeekens, and R. Wu, Quantification of tunicamycin-induced protein expression and N-glycosylation changes in yeast. *Analyst*, 2016. 141(12): p. 3737-45.
45. Karagöz, G.E., D. Acosta-Alvear, and P. Walter, The Unfolded Protein Response: Detecting and Responding to Fluctuations in the Protein-Folding Capacity of the Endoplasmic Reticulum. *Cold Spring Harb Perspect Biol*, 2019. 11(9).
46. Mannan, M.A., et al., An ire1-phk1 chimera reveals a dispensable role of autokinase activity in endoplasmic reticulum stress response. *J Mol Biol*, 2013. 425(12): p. 2083-99.
47. Lee, K.P., et al., Structure of the dual enzyme Ire1 reveals the basis for catalysis and regulation in nonconventional RNA splicing. *Cell*, 2008. 132(1): p. 89-100.
48. Korennykh, A.V., et al., The unfolded protein response signals through high-order assembly of Ire1. *Nature*, 2009. 457(7230): p. 687-93.
49. Thomson, D.D., et al., Contact-induced apical asymmetry drives the thigmotropic responses of *Candida albicans* hyphae. *Cell Microbiol*, 2015. 17(3): p. 342-54.
50. Desai, J.V., *Candida albicans* Hyphae: From Growth Initiation to Invasion. *J Fungi (Basel)*, 2018. 4(1).
51. Vila, T., et al., Targeting *Candida albicans* filamentation for antifungal drug development. *Virulence*, 2017. 8(2): p. 150-158.
52. Rajendran, R., et al., Biofilm formation is a risk factor for mortality in patients with *Candida albicans* bloodstream infection-Scotland, 2012-2013. *Clin Microbiol Infect*, 2016. 22(1): p. 87-93.
53. Lohse, M.B., et al., Development and regulation of single- and multi-species *Candida albicans* biofilms. *Nat Rev Microbiol*, 2018. 16(1): p. 19-31.
54. Nobile, C.J. and A.D. Johnson, *Candida albicans* Biofilms and Human Disease. *Annu Rev Microbiol*, 2015. 69: p. 71-92.
55. Ponde, N.O., et al., *Candida albicans* biofilms and polymicrobial interactions. *Crit Rev Microbiol*, 2021. 47(1): p. 91-111.
56. Jost, L.M., J.M. Kirkwood, and T.L. Whiteside, Improved short- and long-term XTT-based colorimetric cellular cytotoxicity assay for melanoma and other tumor cells. *J Immunol Methods*, 1992. 147(2): p. 153-65.
57. Kuhn, D.M., et al., Uses and limitations of the XTT assay in studies of *Candida* growth and metabolism. *J Clin Microbiol*, 2003. 41(1): p. 506-8.
58. Xiong, J., et al., Geldanamycin confers fungicidal properties to azole by triggering the activation of succinate dehydrogenase. *Life Sci*, 2024. 348: p. 122699.
59. O'Meara, T.R., et al., Global proteomic analyses define an environmentally contingent Hsp90 interactome and reveal chaperone-dependent regulation of stress granule proteins and the R2TP complex in a fungal pathogen. *PLoS Biol*, 2019. 17(7): p. e3000358.
60. Rosenberg, A., et al., Antifungal tolerance is a subpopulation effect distinct from resistance and is associated with persistent candidemia. *Nat Commun*, 2018. 9(1): p. 2470.
61. Li, W., et al., Calcium-calcineurin signaling pathway in *Candida albicans*: A potential drug target. *Microbiol Res*, 2021. 249: p. 126786.
62. Rios, E.I., I.L. Hunsberger, and J.L. Johnson, Insights into Hsp90 mechanism and in vivo functions learned from studies in the yeast, *Saccharomyces cerevisiae*. *Front Mol Biosci*, 2024. 11: p. 1325590.
63. Schwarz, D.S. and M.D. Blower, The endoplasmic reticulum: structure, function and response to cellular signaling. *Cell Mol Life Sci*, 2016. 73(1): p. 79-94.
64. Li, Y., Y. Zhang, and L. Lu, Calcium signaling pathway is involved in non-CYP51 azole resistance in *Aspergillus fumigatus*. *Med Mycol*, 2019. 57(Supplement_2): p. S233-S238.

65. Xiong, J., H. Lu, and Y. Jiang, Mechanisms of Azole Potentiation: Insights from Drug Repurposing Approaches. *ACS Infect Dis*, 2025. 11(2): p. 305-322..

Disclaimer/Publisher's Note: The statements, opinions and data contained in all publications are solely those of the individual author(s) and contributor(s) and not of MDPI and/or the editor(s). MDPI and/or the editor(s) disclaim responsibility for any injury to people or property resulting from any ideas, methods, instructions or products referred to in the content.